

MIT-CTP-2978  
May 2000

# Perturbative renormalization of the first two moments of non-singlet quark distributions with overlap fermions

Stefano Capitani

*Center for Theoretical Physics, Laboratory for Nuclear Science  
Massachusetts Institute of Technology  
77 Massachusetts Ave., Cambridge, MA 02139, USA*

E-mail: stefano@mitlns.mit.edu

---

## Abstract

Using the overlap-Dirac operator proposed by Neuberger, we have computed in lattice QCD the one-loop renormalization factors of ten operators which measure the lowest two moments of unpolarized and polarized non-singlet quark distributions. These factors are necessary to extract physical numbers from Monte Carlo simulations made with overlap fermions.

An exact chiral symmetry is maintained in all our results, and the renormalization constants of corresponding unpolarized and polarized operators which differ by a  $\gamma_5$  matrix have the same value. We have considered two lattice representations for each continuum operator. The computations have been carried out using the symbolic language FORM, in a general covariant gauge. In some simple cases they have also been checked by hand.

---

## 1 Introduction

In recent years remarkable progress has been made towards formulations of lattice fermions which have no doublers and possess an exact chiral symmetry without giving up desirable features like flavor symmetry, locality, unitarity or gauge-invariance. The Ginsparg-Wilson relation [1]

$$\gamma_5 D + D \gamma_5 = a \frac{1}{\rho} D \gamma_5 D \quad (1)$$

has been recognized [2] as the fundamental condition in this context, and a Dirac operator  $D$  which satisfies this relation can indeed describe chiral fermions on the lattice. One of the possible solutions of the Ginsparg-Wilson relation has been found by Neuberger [3] starting from the overlap formalism [4]. In the massless case the overlap-Dirac operator is

$$D_N = \frac{1}{a} \rho \left[ 1 + \frac{X}{\sqrt{X^\dagger X}} \right], \quad (2)$$

where

$$X = D_W - \frac{1}{a} \rho \quad (3)$$

in terms of the usual Wilson-Dirac operator

$$D_W = \frac{1}{2} \left[ \gamma_\mu (\nabla_\mu^* + \nabla_\mu) - ar \nabla_\mu^* \nabla_\mu \right], \quad (4)$$

$$\nabla_\mu \psi(x) = \frac{1}{a} \left[ U(x, \mu) \psi(x + a\hat{\mu}) - \psi(x) \right]. \quad (5)$$

In the range  $0 < \rho < 2r$  the right spectrum of massless fermions is obtained [5]. For a quark of bare mass  $m_0$  the overlap-Dirac operator becomes

$$\left( 1 - \frac{1}{2\rho} am_0 \right) D_N + m_0. \quad (6)$$

Since additive mass renormalization is forbidden, one avoids altogether a source of systematic errors that is always present with Wilson fermions [6].

Lüscher has shown [7] that a fermion obeying the Ginsparg-Wilson relation possesses an exact chiral symmetry of the general form

$$\delta\psi = \epsilon \cdot \gamma_5 \left( 1 - \frac{c}{\rho} aD \right) \psi, \quad \delta\bar{\psi} = \epsilon \cdot \bar{\psi} \left( 1 - \frac{1-c}{\rho} aD \right) \gamma_5. \quad (7)$$

A fully legitimate form of global chiral symmetry is thus preserved for finite lattice spacing. The expected value of the global anomaly [7] (which comes from the non-invariance of the fermionic integration measure under the transformations above), the Atiyah-Singer index theorem on the lattice [2] and the chiral Ward identities are then fully attained before taking the continuum limit. Thus, the central point in this framework is not to insist on the lattice form of the canonical chiral transformations (in fact actions satisfying Eq. (1) are not chirally invariant in the canonical sense), but rather be satisfied with a modified form of the chiral symmetry. The Nielsen-Ninomyia theorem [8] is then circumvented altogether, and it is possible to define chiral fermions without doublers or breaking of flavor symmetry or other unpleasant drawbacks. The chiral transformations (7) depend also on the interaction, but this does not forbid the non-perturbative construction of chiral gauge theories on the lattice with exact gauge invariance [9,10]. For recent reviews on the interesting properties of fermions satisfying the Ginsparg-Wilson relation, see Refs. [5,10,11].

We will be interested in the following in performing chiral-invariant computations by using the overlap-Dirac operator (2). This has been proven to be local <sup>1</sup> [12], and although simulations with the Neuberger operator look computationally very demanding, progress is under way [12,13]. There has been activity also on the analytic side, and some 1-loop calculations with overlap fermions have been already carried out [14–17]. The most recent and advanced calculations have featured the relation between the  $\Lambda$  parameter in the lattice scheme defined by the overlap operator and in the  $\overline{\text{MS}}$  scheme [16], and the renormalization factors of the quark bilinears  $\bar{\psi}\Gamma\psi$  [17].

In this paper we present the calculation in lattice QCD of the renormalization factors of a few operators which measure the lowest two moments of non-singlet quark distributions. The generic operators which measure their  $n$ -th moments are  $\bar{\psi}\gamma_\mu D_{\mu_1}\dots D_{\mu_n}\psi$  and  $\bar{\psi}\gamma_\mu\gamma_5 D_{\mu_1}\dots D_{\mu_n}\psi$  for unpolarized and polarized Structure Functions respectively. Contrary to what happens with Wilson fermions, in the present case, thanks to the exact chiral symmetry that we maintain, the renormalization constants for every pair of corresponding unpolarized and polarized operators which differ by a  $\gamma_5$  matrix are the same.

This paper is organized as follows: in Sect. 2 we introduce the various operators that we have studied, in Sect. 3 their renormalization on the lattice is discussed, and in Sect. 4 some details about the perturbative calculations are given. Finally, in Sect. 5 we present our results. In the Appendices one can find the Feynman rules that we have used as well as some analytic results.

---

<sup>1</sup> The locality is not meant here to be strict locality, but in the larger sense that the strength of the interaction decays exponentially with the distance.

## 2 Moments of Structure Functions

The hadronic physics in Deep Inelastic Scattering is contained in the matrix elements of the T-product of the hadronic currents

$$-i \int d^4x e^{iqx} \langle p | T(J_\mu(x) J_\nu(0)) | p \rangle, \quad (8)$$

$q$  being the momentum transfer and  $p$  the target momentum. An operator product expansion on the light cone of the kind

$$J(x)J(0) \sim \sum_{n,i,l} C_l^{n,i}(x^2) x^{\mu_1} \cdots x^{\mu_n} O_{\mu_1 \cdots \mu_n}^{(n,i)}(0) \quad (9)$$

describes the physics in the Bjorken limit, in which scaling is reached and the Structure Functions depend only on the Bjorken variable  $x_B = -q^2/(2p \cdot q)$ . The moments of the Structure Functions, which measure the moments of quark distributions, are directly connected to the forward matrix elements of the local operators appearing in the light-cone expansion. Since the divergence of the Wilson coefficients is governed by the twist (dimension minus spin) of the corresponding operators, infinite towers of operators of increasing dimension and spin but with the same twist (dimension minus spin) appear at a given order in  $1/q^2$ . The dominant contribution is given by twist two, which in the flavor non-singlet case means the symmetric traceless operators

$$O_{\mu\mu_1 \cdots \mu_n} = \bar{\psi} \gamma_{\{\mu} D_{\mu_1} \cdots D_{\mu_n\}} \frac{\lambda^a}{2} \psi \quad (10)$$

$$O_{\mu\mu_1 \cdots \mu_n}^{(5)} = \bar{\psi} \gamma_{\{\mu} \gamma_5 D_{\mu_1} \cdots D_{\mu_n\}} \frac{\lambda^a}{2} \psi, \quad (11)$$

where  $\lambda^a$  are flavor matrices (which in the following will be omitted and implicitly understood). These operators measure the moment of unpolarized and polarized Structure Functions respectively, that is the moments  $\langle x_B^n \rangle$  of quark momentum distributions and the moments  $\langle (\Delta x_B)^n \rangle$  of quark helicity distributions, at leading twist. Higher-twist operators give the sub-dominant contributions, and in particular twist-4 operators (which include also 4-fermion operators) measure the  $1/q^2$  corrections to these moments [18].

Since we are considering flavor non-singlet operators, there can be no mixing with operators like  $\text{Tr} \sum_\rho F_{\mu_1\rho} D_{\mu_2} \cdots F_{\rho\mu_n}$  and  $\text{Tr} \sum_\rho \tilde{F}_{\mu_1\rho} D_{\mu_2} \cdots F_{\rho\mu_n}$  which measure the gluon distributions. Mixing with these operators is prohibited even when one considers unquenched calculations. Singlet quark operators instead do mix with gluon operators. For more detailed discussions of Deep Inelastic Scattering on the lattice, see Refs. [19–23].

The operators in the light-cone expansion (9) of which we compute the renormalization factors are the following:

$$O_{v_2,d} = \bar{\psi}\gamma_{\{1}D_4\}\psi \quad (12)$$

$$O_{v_2,e} = \bar{\psi}\gamma_4D_4\psi - \frac{1}{3}\sum_{i=1}^3\bar{\psi}\gamma_iD_i\psi, \quad (13)$$

which measure the first moment of quark momentum distributions,

$$O_{a_2,d} = \bar{\psi}\gamma_{\{1}\gamma_5D_4\}\psi \quad (14)$$

$$O_{a_2,e} = \bar{\psi}\gamma_4\gamma_5D_4\psi - \frac{1}{3}\sum_{i=1}^3\bar{\psi}\gamma_i\gamma_5D_i\psi, \quad (15)$$

which measure the first moment of quark helicity distributions,

$$O_{v_3,d} = \bar{\psi}\gamma_{\{4}D_1D_2\}\psi \quad (16)$$

$$O_{v_3,e} = \bar{\psi}\gamma_{\{4}D_1D_1\}\psi - \frac{1}{2}\sum_{i=2}^3\bar{\psi}\gamma_{\{4}D_iD_i\}\psi, \quad (17)$$

which measure the second moment of quark momentum distributions, and

$$O_{a_3,d} = \bar{\psi}\gamma_{\{4}\gamma_5D_1D_2\}\psi \quad (18)$$

$$O_{a_3,e} = \bar{\psi}\gamma_{\{4}\gamma_5D_1D_1\}\psi - \frac{1}{2}\sum_{i=2}^3\bar{\psi}\gamma_{\{4}\gamma_5D_iD_i\}\psi, \quad (19)$$

which measure the second moment of quark helicity distributions. Symmetrization in all Lorentz indices is understood. We use  $D = \vec{D} - \overleftarrow{D}$ , with the following lattice discretizations:

$$\vec{D}_\mu \psi(x) = \frac{1}{2a} \left[ U(x, \mu) \psi(x + a\hat{\mu}) - U^\dagger(x - a\hat{\mu}, \mu) \psi(x - a\hat{\mu}) \right] \quad (20)$$

$$\bar{\psi}(x) \overleftarrow{D}_\mu = \frac{1}{2a} \left[ \bar{\psi}(x + a\hat{\mu}) U^\dagger(x, \mu) - \bar{\psi}(x - a\hat{\mu}) U(x - a\hat{\mu}, \mu) \right]. \quad (21)$$

We have chosen the Lorentz indices of each operator appearing in the continuum expansion in two different ways, so that they fall in two different representations of the hypercubic group (the symmetry group of the lattice, remnant of the Lorentz symmetry), and on the lattice they will then renormalize in a different way. The representations where the indices are all different from each other are least likely to mix with other operators, however one needs more components of the hadron momentum different from zero when

simulating the corresponding matrix elements, and this can lead to more lattice artifacts. Sometimes one of the representations can be easier to handle in practice, depending on the trade-off between the amount of mixing and the number of non-zero momentum components. For example, in the case of the second moment the operator (16) is multiplicatively renormalized, but it can be more advantageous to use the other representation (operator (17)) when it is important that fewer components of the momenta are different from zero, although in this case one has then to deal with a mixing.

The operator (17) (together with the corresponding polarized (19)) is the only one in the list above that is not multiplicatively renormalized on the lattice. What happens is that that the two operators

$$O_A = \bar{\psi}\gamma_4 D_1 D_1 \psi - \frac{1}{2} \sum_{i=2}^3 \bar{\psi}\gamma_4 D_i D_i \psi, \quad (22)$$

$$O_B = \bar{\psi}\gamma_1 D_4 D_1 \psi + \bar{\psi}\gamma_1 D_1 D_4 \psi - \frac{1}{2} \sum_{i=2}^3 \bar{\psi}\gamma_i D_4 D_i \psi - \frac{1}{2} \sum_{i=2}^3 \bar{\psi}\gamma_i D_i D_4 \psi, \quad (23)$$

which are not symmetrized in their indices, do not receive the same 1-loop corrections on the lattice [20], and so the operator (17),

$$O_{v_3,e} = \frac{1}{3} (O_A + O_B), \quad (24)$$

does not go into itself under lattice renormalization, because the symmetric combination is lost. In the polarized case, an analogous situation occurs for

$$O_{A^5} = \bar{\psi}\gamma_4\gamma_5 D_1 D_1 \psi - \frac{1}{2} \sum_{i=2}^3 \bar{\psi}\gamma_4\gamma_5 D_i D_i \psi, \quad (25)$$

$$O_{B^5} = \bar{\psi}\gamma_1\gamma_5 D_4 D_1 \psi + \bar{\psi}\gamma_1\gamma_5 D_1 D_4 \psi - \frac{1}{2} \sum_{i=2}^3 \bar{\psi}\gamma_i\gamma_5 D_4 D_i \psi - \frac{1}{2} \sum_{i=2}^3 \bar{\psi}\gamma_i\gamma_5 D_i D_4 \psi. \quad (26)$$

A detailed discussion of these effects can be found in Sect. 5.

We mention that for the second moment there exists also a third independent lattice representation, in which all indices are equal. However, it mixes with a lower dimensional operator with a power-divergent coefficient ( $\sim 1/a^2$ ), and so we do not consider it here.

### 3 Renormalization

To relate the numbers obtained from Monte Carlo simulations to physical continuum quantities, a lattice renormalization of the relevant matrix elements is necessary. The connection is given by

$$\langle O_i^{\text{cont}} \rangle = \sum_j \left( \delta_{ij} - \frac{g_0^2}{16\pi^2} (R_{ij}^{\text{lat}} - R_{ij}^{\text{cont}}) \right) \cdot \langle O_j^{\text{lat}} \rangle, \quad (27)$$

where

$$\langle O_i^{\text{cont,lat}} \rangle = \sum_j \left( \delta_{ij} + \frac{g_0^2}{16\pi^2} R_{ij}^{\text{cont,lat}} \right) \cdot \langle O_j^{\text{tree}} \rangle \quad (28)$$

are the continuum and lattice 1-loop expressions respectively, and the tree-level matrix element is the same in both cases. The differences  $\Delta R_{ij} = R_{ij}^{\text{lat}} - R_{ij}^{\text{cont}}$  enter then in the renormalization factors

$$Z_{ij}(a\mu, g_0) = \delta_{ij} - \frac{g_0^2}{16\pi^2} \Delta R_{ij}(a\mu) \quad (29)$$

which connect the lattice to the continuum. These renormalization factors are independent of the state, depend only on the scale  $a\mu$  and are gauge-invariant. Using them, a matrix element obtained from Monte Carlo simulations can be renormalized to a continuum scheme.

Although there are in principle also non-perturbative methods with which one can determine the renormalization factors, perturbation theory is still important. In fact, it can happen that for some operators a window for the non-perturbative signal is difficult to obtain, and then perturbation theory remains the only possibility of computing the relevant renormalization factors. For the Neuberger operator, extracting the non-perturbative renormalization factors in addition to simulating the bare matrix elements could turn out to be computationally very expensive. In general, perturbative lattice renormalization is important as a hint and a guide for non-perturbative renormalization studies, and even more when mixings are present, which are generally more intricate than in the continuum case, and more transparent when looked at in perturbation theory, especially if some amounts of mixings are small. Perturbative renormalization can in any case be very useful in checking and understanding results obtained with non-perturbative methods.

In the continuum we renormalize the operators in the  $\overline{\text{MS}}$  scheme. As perturbative renormalization condition on the lattice we impose that the 1-loop

amputated matrix elements at a certain reference scale  $\mu$  are equal to the corresponding bare tree-level quantities. For lattice matrix elements of multiplicatively renormalized operators computed between one-quark states this condition means

$$\begin{aligned} \langle p|O^{\text{lat}}(\mu)|p\rangle\Big|_{p^2=\mu^2} &= Z_O(a\mu, g_0) \cdot Z_\psi^{-1}(a\mu, g_0) \cdot \langle p|O^{(0)}(a)|p\rangle\Big|_{p^2=\mu^2}^{1\text{-loop}} \\ &= \langle p|O^{(0)}(a)|p\rangle\Big|_{p^2=\mu^2}^{\text{tree}}, \end{aligned} \quad (30)$$

where  $Z_\psi$  is the wave-function renormalization, computed from the quark self-energy.

The 1-loop lattice matrix elements of the operators we consider here, which are at most logarithmically divergent, will have the form

$$\begin{aligned} \langle p|O^{(0)}(a)|p\rangle\Big|^{1\text{-loop}} &= \langle p|O^{(0)}(a)|p\rangle\Big|^{\text{tree}} \times \\ &\quad \left(1 + \frac{g_0^2}{16\pi^2} C_F (\gamma_O \log a^2 p^2 + V_O + T_O + 2S)\right), \end{aligned} \quad (31)$$

where  $V_O$  is the finite contribution of the vertex and sails diagrams (a, b and c in Fig. 1),  $T_O$  refers to the tadpole arising from the operator (d in Fig. 1),  $S$  is the finite contribution (proportional to  $i\not{p}$ ) of the quark self-energy of one leg, including the leg tadpole (e and g, or f and h, in Fig. 1), and  $C_F = \frac{N_c^2 - 1}{2N_c}$ . The  $Z_O$  factor for an operator  $O$  will then be given by

$$Z_O(a\mu, g_0) = 1 - \frac{g_0^2}{16\pi^2} C_F \left(\gamma_O \log a^2 \mu^2 + B_O\right), \quad (32)$$

with

$$B_O = V_O + T_O + S. \quad (33)$$

We will call ‘‘proper’’ contributions the ones that exclude the self-energy diagrams. They correspond to the diagrams a-d in Fig. 1.

Although the theory defined by the overlap-Dirac operator (2) has an exact chiral symmetry and no lattice artifacts of order  $a$  are present in the action, matrix elements of operators still possess corrections of order  $a$  and therefore they need to be improved. The improved operator corresponding to  $\bar{\psi}\gamma_{\{\mu}D_{\mu_1}\cdots D_{\mu_n\}}\psi$  is [24]

$$\bar{\psi}\left(1 - \frac{1}{2}aD_N\right)\gamma_{\{\mu}D_{\mu_1}\cdots D_{\mu_n\}}\left(1 - \frac{1}{2}aD_N\right)\psi, \quad (34)$$



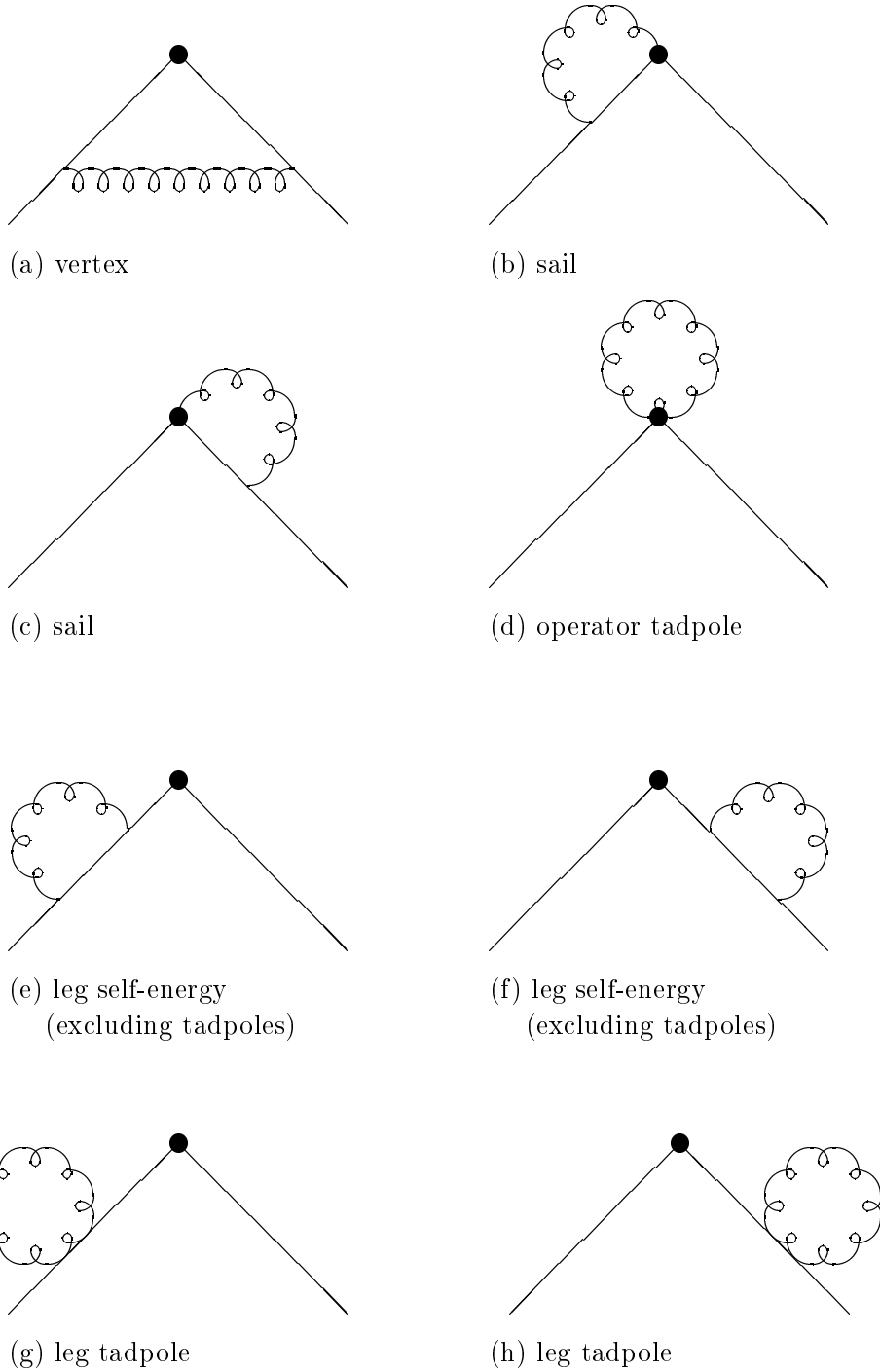


Fig. 1. The graphs contributing to the 1-loop renormalization factors of the matrix elements  $\langle p|O|p\rangle$ . The operator insertion is indicated by a circle.

and the big bonus with overlap fermions is that the renormalization factors for the improved operator and for the unimproved operator without the rotations ( $1 - \frac{1}{2}aD_N$ ) are the same. What happens is that in 1-loop amplitudes a factor  $D_N$  can combine with a quark propagator, but since it has an  $a$  in front and (contrary to the Wilson case) there is no  $1/a$  factor in the propagator, as additive mass renormalization is forbidden by chiral symmetry, the contribution of  $D_N$  to the renormalization factors is zero [17]. Thus, we can simulate the improved operator (34) and renormalize it as if it were the unimproved operator, which saves a lot in the perturbative calculations.

Chiral symmetry, in addition to avoiding the extrapolations to zero quark mass in the simulations, gives also useful constraints on the mixing patterns and on the values of the renormalization factors. In general, mixings that in the Wilson case were allowed by the breaking of chirality are now forbidden, although this has less relevance here than in other problems like in weak interactions [25]. An important consequence here is that, similarly to what happens in the case of the bilinears where we have  $Z_S = Z_P$  and  $Z_V = Z_A$  [17], chiral symmetry forces pairs of corresponding unpolarized and polarized operators, like  $O_{v_2,d}$  and  $O_{a_2,d}$ , to have the same renormalization constants <sup>2</sup>.

## 4 The computations

The interaction vertices and the propagator of the overlap-Dirac operator are much more complicated than the ones in the Wilson formulation, and this causes the computations to be rather cumbersome (see Appendices). Computer programs need then to be introduced, and we have performed the calculations using an ensemble of routines written in the symbolic manipulation language FORM. These routines are an extension of the ones used to do calculations with the Wilson action in various occasions [23,26].

The outputs of the FORM codes, which correspond to the results of the analytic calculations, are fed to Fortran programs which perform the numerical integrations. To treat the divergent integrals we use the Kawai method [27], in which they are split in integrals independent of external momenta plus continuum integrals. Divergent lattice integrals which contain both gluon and overlap-quark propagators are reduced to divergent integrals containing only gluon propagators, which are computed in a exact way as in [28], plus a finite rest.

---

<sup>2</sup> This is strictly true for improved operators like in Eq. (34), which transform like chiral multiplets, but since they have the same renormalization constants as the unimproved operators, these symmetry relations are preserved.

Many checks have been performed on our results. We did the computations in a general covariant gauge <sup>3</sup>, and the cancellations of the gauge-dependent parts between the continuum scheme and the lattice results is a strong check on the good behavior of the FORM codes, as well as of the integration routines.

We have used the codes to compute also the renormalization constants for all quark bilinears, and we agree with the results given in Feynman-gauge by Alexandrou et al. [17], as well as with their self-energy. In the case of the leg tadpole and of the vertex graph of the scalar current  $\bar{\psi}\psi$  we have also made the computations entirely by hand (although only in the Feynman gauge), and successfully checked them against the FORM output expressions. These analytic results are reported in Appendix B. We tried to do a calculation by hand for a first moment operator and for the rest of the leg self-energy, but they involved a huge amount of manipulations. We rely also on the vast amount of results which have been produced in different occasions using these FORM codes limited to the Wilson formulation [23,26], and these results have by now a certain number of cross-checks. With overlap fermions we need to introduce a new propagator and new vertices, but the operators are unaltered, and the same Wilson expressions for their expansion in  $a$  can be used here. Many of the routines (for example the gamma algebra reduction) are also exactly the same as in the Wilson case.

We checked in all cases that the polarized operators have the same  $Z$ s as the corresponding unpolarized operators. This is a rather strong check, as the analytic results are widely different for the two cases, and it is only after performing the numerical integrations and seeing that the difference of the two results is much smaller than the precision of our integrals that we are able to say that the renormalization factors are indeed equal. Finally, since our codes are able to do calculations both in Dimensional Regularization and using a mass regularization, we also checked that using two different intermediate regularizations while treating the divergences with the Kawai method [27] we get the same results.

We obtain the  $B_O$  constants with 5 digits after the decimal points, by doing the numerical integrations on a  $40^4$  regular grid and using the method proposed by Lüscher and Weisz in [29] to accelerate convergence. We have checked that these digits do not vary when a  $60^4$  integration grid is used. In any case, to get more significant digits, grids of  $80^4$  or  $100^4$  points would still not be enough, and they would require an enormous computational effort, as a typical FORM output for the second moment operators already contains thousands of terms.

---

<sup>3</sup> The gluon propagator that we use is

$$G_{\mu\nu}(k) = \frac{1}{4 \sum_{\rho} \sin^2 \frac{k_{\rho}}{2}} \left( \delta_{\mu\nu} - (1 - \alpha) \frac{4 \sin \frac{k_{\mu}}{2} \sin \frac{k_{\nu}}{2}}{4 \sum_{\lambda} \sin^2 \frac{k_{\lambda}}{2}} \right). \quad (35)$$

Comparing our results for the self-energy and the bilinears with the numbers in Ref. [17], we can see that a few times a difference of one unit on the fifth digit can be noticed, and this agrees with our estimate of errors. In that paper the results are given in terms of the constants  $b = \frac{B}{16\pi^2}$ , and this explains the presence of two more significant digits after the decimal point.

## 5 Results

We give in this Section the renormalization factors of the operators considered in this work. That these factors are identical for pairs of corresponding unpolarized and polarized operators has been explicitly verified for all operators. We give then the numerical results only for the unpolarized operators, for  $r = 1$ .

We first consider the 1-loop contributions of the proper diagrams (a-d in Fig. 1), which for the operators that do not mix are

$$\begin{aligned}
O_{v_2,d}^{\text{proper}} &= \frac{g_0^2}{16\pi^2} C_F \left[ \left( \frac{5}{3} + (1 - \alpha) \right) \log a^2 p^2 \right. \\
&\quad \left. + V_{v_2,d}^{\alpha=1} - (1 - \alpha) 6.850272 + T_{v_2,d} \right] O_{v_2,d}^{\text{tree}}, \\
O_{v_2,e}^{\text{proper}} &= \frac{g_0^2}{16\pi^2} C_F \left[ \left( \frac{5}{3} + (1 - \alpha) \right) \log a^2 p^2 \right. \\
&\quad \left. + V_{v_2,e}^{\alpha=1} - (1 - \alpha) 6.850272 + T_{v_2,e} \right] O_{v_2,e}^{\text{tree}}, \\
O_{v_3,d}^{\text{proper}} &= \frac{g_0^2}{16\pi^2} C_F \left[ \left( \frac{19}{6} + (1 - \alpha) \right) \log a^2 p^2 \right. \\
&\quad \left. + V_{v_3,d}^{\alpha=1} - (1 - \alpha) 7.369693 + T_{v_3,d} \right] O_{v_3,d}^{\text{tree}}.
\end{aligned} \tag{36}$$

The contributions of the sails and vertices,  $V_O$ , have been for convenience separated in the Feynman gauge results ( $V_{v_2,d}^{\alpha=1}$ ,  $V_{v_2,e}^{\alpha=1}$  and  $V_{v_3,d}^{\alpha=1}$ ), tabulated in Table 1 for various values of the parameter  $\rho$ , and the remaining parts proportional to  $(1 - \alpha)$ , which are instead independent of  $\rho$ . The analytic expressions of the latter are very complicated functions of  $\rho$  containing thousands of terms, and the numerical cancellation of this dependence is a rather non-trivial check of our computations. These numbers are also independent of the lattice representation, and furthermore they have the same value as with the Wilson action [26], so they seem to be to a certain extent independent of the particular fermion action chosen.

$\rho$	$V_{v_2,d}^{\alpha=1} = V_{a_2,d}^{\alpha=1}$	$V_{v_2,e}^{\alpha=1} = V_{a_2,e}^{\alpha=1}$	$V_{v_3,d}^{\alpha=1} = V_{a_3,d}^{\alpha=1}$
0.2	-3.77889	-3.50634	-7.57984
0.3	-3.71038	-3.41915	-7.45926
0.4	-3.65209	-3.34178	-7.35607
0.5	-3.60037	-3.27058	-7.26432
0.6	-3.55327	-3.20357	-7.18078
0.7	-3.50959	-3.13952	-7.10341
0.8	-3.46851	-3.07762	-7.03088
0.9	-3.42946	-3.01727	-6.96221
1.0	-3.39203	-2.95803	-6.89668
1.1	-3.35589	-2.89955	-6.83375
1.2	-3.32077	-2.84155	-6.77296
1.3	-3.28647	-2.78380	-6.71398
1.4	-3.25281	-2.72610	-6.65650
1.5	-3.21964	-2.66827	-6.60029
1.6	-3.18685	-2.61015	-6.54513
1.7	-3.15430	-2.55162	-6.49084
1.8	-3.12190	-2.49255	-6.43729

Table 1

The Feynman-gauge constants  $V_O^{\alpha=1}$  for the multiplicatively renormalized operators.

The contributions  $T_O$  of the operator tadpoles (d in Fig. 1) are shown in Table 2, which contains also their results for the other operator,  $O_{v_3,e}$ . However, since this operator is not multiplicatively renormalized on the lattice, we consider in its place the two operators  $O_A$  and  $O_B$  introduced in Sect. 2. They mix with each other and we can write their renormalization as <sup>4</sup>

$$\begin{aligned}
\widehat{O}_A &= Z_{AA}O_A + Z_{AB}O_B \\
\widehat{O}_B &= Z_{BA}O_A + Z_{BB}O_B.
\end{aligned}
\tag{37}$$

In terms of the bare operators  $O_A$  and  $O_B$ , the renormalized operator  $\widehat{O}_{v_3,e}$

<sup>4</sup> In Refs. [21] another choice for the two operators that mix was made, and  $O_{v_3,e}$  and an operator of mixed symmetry were considered instead of  $O_A$  and  $O_B$ .

operator	operator tadpole
$O_{v_2,d}, O_{a_2,d}$	$T_{v_2,d} = T_{a_2,d} = -16\pi^2 \frac{Z_0}{2} \left(1 - \frac{1}{4}(1 - \alpha)\right)$
$O_{v_2,e}, O_{a_2,e}$	$T_{v_2,e} = T_{a_2,e} = -16\pi^2 \frac{Z_0}{2} \left(1 - \frac{1}{4}(1 - \alpha)\right)$
$O_{v_3,d}, O_{a_3,d}$	$T_{v_3,d} = T_{a_3,d} = 16\pi^2 \left(-Z_0 + (1 - \alpha) \frac{Z_0}{6}\right)$
$O_{v_3,e}, O_{a_3,e}$	$T_{AA} = T_{A^5A^5} = 16\pi^2 \left(-2Z_0 + \frac{1}{8} + (1 - \alpha) \left(Z_0 - \frac{1}{8}\right)\right)$ $T_{AB} = T_{A^5B^5} = 0$ $T_{BA} = T_{B^5A^5} = 0$ $T_{BB} = T_{B^5B^5} = 16\pi^2 \left(-Z_0 + (1 - \alpha) \frac{Z_0}{6}\right)$

Table 2

The operator tadpoles for the various operators, where  $Z_0 = 0.154933390231$ .

appearing in the DIS light-cone expansion will be

$$\hat{O}_{v_3,e} = \frac{1}{3}(\hat{O}_A + \hat{O}_B) = \frac{1}{3}(Z_{AA} + Z_{BA})O_A + \frac{1}{3}(Z_{AB} + Z_{BB})O_B, \quad (38)$$

and since on the lattice  $Z_{AA} + Z_{BA} \neq Z_{AB} + Z_{BB}$ , the result is that  $O_{v_3,e}$  is not multiplicatively renormalized. In fact, the 1-loop contributions coming from the proper diagrams are in this case

$$\begin{aligned}
O_A^{\text{proper}} &= \frac{g_0^2}{16\pi^2} C_F \left[ \left(\frac{7}{6} + (1 - \alpha)\right) \log a^2 p^2 \right. \\
&\quad \left. + V_{AA}^{\alpha=1} - (1 - \alpha) 8.685568 + T_{AA} \right] O_A^{\text{tree}} \\
&\quad + \frac{g_0^2}{16\pi^2} C_F \left[ \log a^2 p^2 + V_{AB}^{\alpha=1} + \frac{1}{3}(1 - \alpha) + T_{AB} \right] O_B^{\text{tree}} \\
O_B^{\text{proper}} &= \frac{g_0^2}{16\pi^2} C_F \left[ 2 \log a^2 p^2 + V_{BA}^{\alpha=1} + \frac{2}{3}(1 - \alpha) + T_{BA} \right] O_A^{\text{tree}} \\
&\quad + \frac{g_0^2}{16\pi^2} C_F \left[ \left(\frac{13}{6} + (1 - \alpha)\right) \log a^2 p^2 \right. \\
&\quad \left. + V_{BB}^{\alpha=1} - (1 - \alpha) 7.703026 + T_{BB} \right] O_B^{\text{tree}}, \quad (39)
\end{aligned}$$

where the finite contributions of vertex and sails in the Feynman gauge are shown in Table 3.

We stress again that this mixing is a pure lattice effect, deriving from the

$\rho$	$V_{AA}^{\alpha=1} = V_{A^5A^5}^{\alpha=1}$	$V_{BA}^{\alpha=1} = V_{B^5A^5}^{\alpha=1}$	$V_{AB}^{\alpha=1} = V_{A^5B^5}^{\alpha=1}$	$V_{BB}^{\alpha=1} = V_{B^5B^5}^{\alpha=1}$
0.2	22.83163	-36.93402	-13.77026	10.81988
0.3	13.03570	-24.07048	-8.80836	4.50553
0.4	8.39467	-17.86369	-6.43263	1.50207
0.5	5.76489	-14.27357	-5.06826	-0.20460
0.6	4.11604	-11.96971	-4.19847	-1.27644
0.7	3.01383	-10.38860	-3.60511	-1.99319
0.8	2.24472	-9.25173	-3.18071	-2.49274
0.9	1.69205	-8.40616	-2.86648	-2.85062
1.0	1.28701	-7.76116	-2.62765	-3.11148
1.1	0.98657	-7.25963	-2.44241	-3.30329
1.2	0.76254	-6.86397	-2.29645	-3.44445
1.3	0.59577	-6.54843	-2.18002	-3.54747
1.4	0.47280	-6.29483	-2.08624	-3.62114
1.5	0.38399	-6.08998	-2.01015	-3.67183
1.6	0.32223	-5.92413	-1.94810	-3.70420
1.7	0.28218	-5.78989	-1.89733	-3.72177
1.8	0.25980	-5.68156	-1.85572	-3.72723

Table 3

The Feynman-gauge constants  $V_O^{\alpha=1}$  for the operators  $O_A$  and  $O_B$  related to  $O_{v_3,e}$ .

breaking of the Lorentz group to the hypercubic group. In the continuum we do have  $Z_{AA} + Z_{BA} = Z_{AB} + Z_{BB}$ , and thus the operator  $O_{v_3,e}$  is multiplicatively renormalized, and has the same  $Z$  as the operator with different indices  $O_{v_3,d}$ , as they both belong to the same representation of the Lorentz group. We remind also that in the polarized case one encounters exactly the same situation with the same numerical results, i.e.  $Z_{AA} = Z_{A^5A^5}$ ,  $Z_{AB} = Z_{A^5B^5}$  etc., as we have explicitly verified.

To complete the computation of the renormalization factors, we have now to add to the proper diagrams the 1-loop amplitudes of the self-energy and tadpole of one leg which are proportional to  $i\hat{p}$ ,

$$\Sigma_1 = \frac{g_0^2}{16\pi^2} C_F \left[ \alpha \log a^2 p^2 + S^{\alpha=1} + (1 - \alpha) 4.792010 \right], \quad (40)$$

$\rho$	S	$\rho$	S	$\rho$	S
0.2	-240.59963	0.8	-49.99380	1.4	-23.76598
0.3	-155.41069	0.9	-43.10649	1.5	-21.50111
0.4	-112.98999	1.0	-37.63063	1.6	-19.53531
0.5	-87.65282	1.1	-33.17935	1.7	-17.81537
0.6	-70.84428	1.2	-29.49505	1.8	-16.29999
0.7	-58.90122	1.3	-26.39961	1.9	-14.95658

Table 4  
1-loop results for the quark self-energy (including the leg tadpole).

where the Feynman-gauge finite results  $S^{\alpha=1}$  are given in Table 4. Putting everything together, we get the expressions of the renormalized operators on the lattice for overlap fermions, which for  $\rho = 1$  are:

$$\begin{aligned}
\widehat{O}_{v_2,d} &= \left[ 1 - \frac{g_0^2}{16\pi^2} C_F \left( \frac{8}{3} \log a^2 \mu^2 - 53.25571 + (1 - \alpha) \right) \right] O_{v_2,d}^{\text{tree}} \\
\widehat{O}_{v_2,e} &= \left[ 1 - \frac{g_0^2}{16\pi^2} C_F \left( \frac{8}{3} \log a^2 \mu^2 - 52.82171 + (1 - \alpha) \right) \right] O_{v_2,e}^{\text{tree}} \\
\widehat{O}_{v_3,d} &= \left[ 1 - \frac{g_0^2}{16\pi^2} C_F \left( \frac{25}{6} \log a^2 \mu^2 - 68.99341 + \frac{3}{2} (1 - \alpha) \right) \right] O_{v_3,d}^{\text{tree}} \\
\widehat{O}_{v_3,e} &= \frac{1}{3} \left[ 1 - \frac{g_0^2}{16\pi^2} C_F \left( \frac{25}{6} \log a^2 \mu^2 - 73.29777 + \frac{3}{2} (1 - \alpha) \right) \right] O_A^{\text{tree}} \quad (41) \\
&\quad + \frac{1}{3} \left[ 1 - \frac{g_0^2}{16\pi^2} C_F \left( \frac{25}{6} \log a^2 \mu^2 - 67.83586 + \frac{3}{2} (1 - \alpha) \right) \right] O_B^{\text{tree}}.
\end{aligned}$$

We give here for comparison the numerical values obtained with the usual Wilson action, without any improvement. We have computed them again and checked them with the results in the literature [19–23,26]. In this case however chiral invariance is broken and the renormalization factors for the unpolarized operators

$$\begin{aligned}
\widehat{O}_{v_2,d}^{\text{Wilson}} &= \left[ 1 - \frac{g_0^2}{16\pi^2} C_F \left( \frac{8}{3} \log a^2 \mu^2 - 3.16486 + (1 - \alpha) \right) \right] O_{v_2,d}^{\text{tree}} \\
\widehat{O}_{v_2,e}^{\text{Wilson}} &= \left[ 1 - \frac{g_0^2}{16\pi^2} C_F \left( \frac{8}{3} \log a^2 \mu^2 - 1.88259 + (1 - \alpha) \right) \right] O_{v_2,e}^{\text{tree}}
\end{aligned}$$



$$\begin{aligned}
\widehat{O}_{v_3,d}^{\text{Wilson}} &= \left[ 1 - \frac{g_0^2}{16\pi^2} C_F \left( \frac{25}{6} \log a^2 \mu^2 - 19.00763 + \frac{3}{2} (1 - \alpha) \right) \right] O_{v_3,d}^{\text{tree}} \\
\widehat{O}_{v_3,e}^{\text{Wilson}} &= \frac{1}{3} \left[ 1 - \frac{g_0^2}{16\pi^2} C_F \left( \frac{25}{6} \log a^2 \mu^2 - 21.78271 + \frac{3}{2} (1 - \alpha) \right) \right] O_A^{\text{tree}} \quad (42) \\
&\quad + \frac{1}{3} \left[ 1 - \frac{g_0^2}{16\pi^2} C_F \left( \frac{25}{6} \log a^2 \mu^2 - 18.46640 + \frac{3}{2} (1 - \alpha) \right) \right] O_B^{\text{tree}}
\end{aligned}$$

differ from the ones of the polarized operators

$$\begin{aligned}
\widehat{O}_{a_2,d}^{\text{Wilson}} &= \left[ 1 - \frac{g_0^2}{16\pi^2} C_F \left( \frac{8}{3} \log a^2 \mu^2 - 4.09933 + (1 - \alpha) \right) \right] O_{a_2,d}^{\text{tree}} \\
\widehat{O}_{a_2,e}^{\text{Wilson}} &= \left[ 1 - \frac{g_0^2}{16\pi^2} C_F \left( \frac{8}{3} \log a^2 \mu^2 - 4.27705 + (1 - \alpha) \right) \right] O_{a_2,e}^{\text{tree}} \\
\widehat{O}_{a_3,d}^{\text{Wilson}} &= \left[ 1 - \frac{g_0^2}{16\pi^2} C_F \left( \frac{25}{6} \log a^2 \mu^2 - 19.56159 + \frac{3}{2} (1 - \alpha) \right) \right] O_{a_3,d}^{\text{tree}} \\
\widehat{O}_{a_3,e}^{\text{Wilson}} &= \frac{1}{3} \left[ 1 - \frac{g_0^2}{16\pi^2} C_F \left( \frac{25}{6} \log a^2 \mu^2 - 22.39940 + \frac{3}{2} (1 - \alpha) \right) \right] O_{A^5}^{\text{tree}} \quad (43) \\
&\quad + \frac{1}{3} \left[ 1 - \frac{g_0^2}{16\pi^2} C_F \left( \frac{25}{6} \log a^2 \mu^2 - 19.25837 + \frac{3}{2} (1 - \alpha) \right) \right] O_{B^5}^{\text{tree}}.
\end{aligned}$$

What one can notice is that the values of the renormalization factors for overlap fermions are in general much larger than for Wilson fermions. This seems to be true for most values of  $\rho$ , and is to trace largely to the quark self-energy and to the operators tadpoles. It can be observed that when in the Wilson formulation one improves the theory by adding the clover term to the action (with  $c_{sw} = 1$ ) and by canceling  $O(a)$  effects on the operators at tree level, the renormalization factors become also somewhat larger, as in the examples below [19,20]:

$$\begin{aligned}
\widehat{O}_{v_2,d}^{\text{Wilson, imp}} &= \left[ 1 - \frac{g_0^2}{16\pi^2} C_F \left( \frac{8}{3} \log a^2 \mu^2 - 15.816 + (1 - \alpha) \right) \right] O_{v_2,d}^{\text{tree}} \\
\widehat{O}_{v_3,d}^{\text{Wilson, imp}} &= \left[ 1 - \frac{g_0^2}{16\pi^2} C_F \left( \frac{25}{6} \log a^2 \mu^2 - 29.815 + \frac{3}{2} (1 - \alpha) \right) \right] O_{v_3,d}^{\text{tree}} \\
\widehat{O}_{v_3,e}^{\text{Wilson, imp}} &= \frac{1}{3} \left[ 1 - \frac{g_0^2}{16\pi^2} C_F \left( \frac{25}{6} \log a^2 \mu^2 - 39.192 + \frac{3}{2} (1 - \alpha) \right) \right] O_A^{\text{tree}} \quad (44) \\
&\quad + \frac{1}{3} \left[ 1 - \frac{g_0^2}{16\pi^2} C_F \left( \frac{25}{6} \log a^2 \mu^2 - 22.141 + \frac{3}{2} (1 - \alpha) \right) \right] O_B^{\text{tree}}.
\end{aligned}$$

One could then speculate whether the large renormalization factors that we have obtained for overlap fermions are related to the fact that the Neuberger action is improved and the  $Z$ s correspond to the ones of improved operators.

A calculation with Wilson fermions with which to compare in this sense our overlap results would be one in which the operators are improved beyond tree level, but although we know in some cases the contributions of the operator counterterms that are needed for the full improvement, unfortunately not all their coefficients are yet determined [26].

We give finally the 1-loop results for the various matrix elements in the  $\overline{\text{MS}}$  scheme, so that one can complete the connection with the continuum as in Eq. (27). In the continuum there is only one renormalization constant for all possible operators (unpolarized and polarized) measuring the first moment, and only one for all possible operators measuring the second moment:

$$\begin{aligned}\widehat{O}_{v_2}^{\overline{\text{MS}}} &= \left[ 1 - \frac{g_0^2}{16\pi^2} C_F \left( \frac{8}{3} \log \frac{p^2}{\mu^2} - \frac{40}{9} + (1 - \alpha) \right) \right] O_{v_2}^{\text{tree}} \\ \widehat{O}_{v_3}^{\overline{\text{MS}}} &= \left[ 1 - \frac{g_0^2}{16\pi^2} C_F \left( \frac{25}{6} \log \frac{p^2}{\mu^2} - \frac{67}{9} + \frac{3}{2} (1 - \alpha) \right) \right] O_{v_3}^{\text{tree}}.\end{aligned}\tag{45}$$

The connection of overlap lattice fermions with the continuum  $\overline{\text{MS}}$  is then given by the gauge-invariant factors

$$\begin{aligned}\widehat{O}_{v_2,d}^{\overline{\text{MS}}} &= \left[ 1 - \frac{g_0^2}{16\pi^2} C_F \left( \frac{8}{3} \log a^2 \mu^2 - 48.81127 \right) \right] O_{v_2,d}^{\text{lat}} \\ \widehat{O}_{v_2,e}^{\overline{\text{MS}}} &= \left[ 1 - \frac{g_0^2}{16\pi^2} C_F \left( \frac{8}{3} \log a^2 \mu^2 - 48.37727 \right) \right] O_{v_2,e}^{\text{lat}} \\ \widehat{O}_{v_3,d}^{\overline{\text{MS}}} &= \left[ 1 - \frac{g_0^2}{16\pi^2} C_F \left( \frac{25}{6} \log a^2 \mu^2 - 61.54897 \right) \right] O_{v_3,d}^{\text{lat}} \\ \widehat{O}_{v_3,e}^{\overline{\text{MS}}} &= \frac{1}{3} \left[ 1 - \frac{g_0^2}{16\pi^2} C_F \left( \frac{25}{6} \log a^2 \mu^2 - 65.85333 \right) \right] O_A^{\text{lat}} \\ &\quad + \frac{1}{3} \left[ 1 - \frac{g_0^2}{16\pi^2} C_F \left( \frac{25}{6} \log a^2 \mu^2 - 60.39142 \right) \right] O_B^{\text{lat}}.\end{aligned}\tag{46}$$

It looks increasingly difficult to go to higher moments, as the number of terms that are present in the FORM outputs and that need to be numerically integrated becomes very large. This has at the moment limited our calculations to second moment operators, but we hope to be able to compute the renormalization of third-moment operators in the near future.

Finally, we remark that all the renormalization constants presented here can be considered as computed in the unquenched case, because we limit ourselves to 1-loop computations with non-singlet quark operators, where internal quark loops never have the chance to come to play.

## Acknowledgment

I have enjoyed stimulating discussions with Robert Edwards and Leonardo Giusti. I would also like to thank Mark Alford for critically reading the manuscript. Both the FORM and Fortran computations have been done at MIT on a few Pentium III PCs running on Linux. This work has been supported in part by the U.S. Department of Energy (DOE) under cooperative research agreement DE-FC02-94ER40818.

## A Feynman rules for the Neuberger operator

We give here the Feynman rules which are needed to perform 1-loop calculations using the overlap-Dirac operator. An explicit derivations of these rules is given in [14,15].

The quark propagator is

$$S(k) = \frac{-i \sum_{\mu} \gamma_{\mu} \sin ak_{\mu}}{2\rho(\omega(k) + b(k))} + \frac{a}{2\rho}, \quad (\text{A.1})$$

where

$$\begin{aligned} \omega(k) &= \frac{1}{a} \sqrt{\sum_{\mu} \sin^2 ak_{\mu} + \left(2r \sum_{\mu} \sin^2 \frac{ak_{\mu}}{2} - \rho\right)^2} \\ b(k) &= \frac{1}{a} \left(2r \sum_{\mu} \sin^2 \frac{ak_{\mu}}{2} - \rho\right). \end{aligned} \quad (\text{A.2})$$

The vertices needed for 1-loop calculations can be entirely given in terms of the vertices of the Wilson action

$$W_{1\mu}(p_1, p_2) = -g_0 \left( i\gamma_{\mu} \cos \frac{a(p_1 + p_2)_{\mu}}{2} + r \sin \frac{a(p_1 + p_2)_{\mu}}{2} \right) \quad (\text{A.3})$$

$$W_{2\mu}(p_1, p_2) = -\frac{1}{2} ag_0^2 \left( -i\gamma_{\mu} \sin \frac{a(p_1 + p_2)_{\mu}}{2} + r \cos \frac{a(p_1 + p_2)_{\mu}}{2} \right) \quad (\text{A.4})$$

(where  $p_1$  and  $p_2$  are the quark momenta flowing in and out of the vertices) and of the quantity

$$X_0(p) = \frac{1}{a} \left( i \sum_{\mu} \gamma_{\mu} \sin ap_{\mu} + 2r \sum_{\mu} \sin^2 \frac{ap_{\mu}}{2} - \rho \right). \quad (\text{A.5})$$

The quark-quark-gluon vertex in the overlap theory has the expression

$$V_{1\mu}(p_1, p_2) = \rho \frac{1}{\omega(p_1) + \omega(p_2)} \times \quad (\text{A.6})$$

$$\left[ W_{1\mu}(p_1, p_2) - \frac{1}{\omega(p_1)\omega(p_2)} X_0(p_2) W_{1\mu}^\dagger(p_1, p_2) X_0(p_1) \right], \quad (\text{A.7})$$

and the quark-quark-gluon-gluon vertex is

$$V_{2\mu\nu}(p_1, p_2) = \delta_{\mu\nu} \rho \frac{1}{\omega(p_1) + \omega(p_2)} \times \quad (\text{A.8})$$

$$\begin{aligned} & \left[ W_{2\mu}(p_1, p_2) - \frac{1}{\omega(p_1)\omega(p_2)} X_0(p_2) W_{2\mu}^\dagger(p_1, p_2) X_0(p_1) \right] \\ & + \frac{1}{2} \rho \frac{1}{\omega(p_1) + \omega(p_2)} \frac{1}{\omega(p_1) + \omega(k)} \frac{1}{\omega(k) + \omega(p_2)} \times \\ & \left[ X_0(p_2) W_{1\mu}^\dagger(p_2, k) W_{1\nu}(k, p_1) + W_{1\mu}(p_2, k) X_0^\dagger(k) W_{1\nu}(k, p_1) \right. \\ & \quad \left. + W_{1\mu}(p_2, k) W_{1\nu}^\dagger(k, p_1) X_0(p_1) \right. \\ & \quad \left. - \frac{\omega(p_1) + \omega(k) + \omega(p_2)}{\omega(p_1)\omega(k)\omega(p_2)} X_0(p_2) W_{1\mu}^\dagger(p_2, k) X_0(k) W_{1\nu}^\dagger(k, p_1) X_0(p_1) \right]. \end{aligned}$$

## B Some analytic results

We give here the analytic results for the leg tadpole and for the vertex of the scalar current, in the Feynman gauge for  $r = 1$ . In order to be able to write them in a compact form it is convenient to introduce the abbreviations

$$M_\lambda = \cos \frac{k_\lambda}{2}, \quad N_\lambda = \sin \frac{k_\lambda}{2}, \quad s_\lambda = \sin k_\lambda, \quad s^2 = \sum_\lambda s_\lambda^2, \quad (\text{B.1})$$

$$b = b(k) = 2 \sum_\lambda \sin^2 \frac{k_\lambda}{2} - \rho, \quad (\text{B.2})$$

$$D = 2\rho(\omega(k) + b(k)), \quad (\text{B.3})$$

$$A = \frac{\omega^2(k)}{\rho^2} = 1 - \frac{4}{\rho} \sum_\lambda \sin^2 \frac{k_\lambda}{2} + \frac{1}{\rho^2} \left( \sum_\lambda \sin^2 k_\lambda + \left( 2 \sum_\lambda \sin^2 \frac{k_\lambda}{2} \right)^2 \right). \quad (\text{B.4})$$

The result for the 1-loop leg tadpole is then given by

$$\begin{aligned}
& \frac{1}{2}g_0^2 \int \frac{d^4k}{2\pi^4} G(k) \left(1 - \frac{4}{\rho}\right) \\
& + g_0^2 \int \frac{d^4k}{2\pi^4} G(k) \frac{1}{\rho^2(1 + \sqrt{A})^2} \times \\
& \quad \sum_{\lambda} \left[ M_{\lambda}^2 + N_{\lambda}^2 + \left(1 + \frac{1}{\sqrt{A}}\right) \left(-s_{\mu}^2 + b(M_{\mu}^2 - N_{\mu}^2)\right) \right. \\
& \quad \quad \left. + \frac{2 + \sqrt{A}}{\rho\sqrt{A}} \left(-b(M_{\lambda}^2 - N_{\lambda}^2) + s^2\right) \right] \\
& + g_0^2 \int \frac{d^4k}{2\pi^4} G^2(k) \frac{1}{\rho^2(1 + \sqrt{A})^2} \times \\
& \quad \sum_{\lambda} \left[ -2s_{\mu}^2 N_{\lambda}^2 + \left(1 + \frac{1}{\sqrt{A}}\right) \left(2s_{\mu}^2(b + 2M_{\mu}^2 - M_{\lambda}^2)\right) \right].
\end{aligned} \tag{B.5}$$

The first term comes from the part of the  $V_2$  vertex (A.8) containing  $W_2$  and  $W_2^{\dagger}$ , and its value for  $\rho = 1$  is

$$g_0^2 \cdot \frac{Z_0}{2} \left(1 - \frac{4}{\rho}\right) \Big|_{\rho=1} = -\frac{g_0^2}{16\pi^2} 36.69915, \tag{B.6}$$

while the 1-loop result for the whole leg tadpole is smaller:

$$-\frac{g_0^2}{16\pi^2} 23.35975. \tag{B.7}$$

Adding now the value  $-\frac{g_0^2}{16\pi^2} 14.27088$  for the diagram e in Fig. 1, which is much harder to compute by hand and would be a very lengthy analytic expression anyway, gives the result  $-\frac{g_0^2}{16\pi^2} 37.63063$  for the complete self-energy in the Feynman gauge for  $\rho = 1$ .

The results for the 1-loop vertex diagram of the scalar operator (the sails are not present in this case) can be written in the form

$$g_0^2 \int \frac{d^4k}{2\pi^4} G(p-k) \frac{1}{(1 + \sqrt{A})^2} \left[ \left(-\frac{s^2}{D^2} + \frac{1}{4\rho^2}\right) \cdot X + \frac{1}{\rho D} \cdot Y \right], \tag{B.8}$$

for small  $p$ , where

$$\begin{aligned}
X = \sum_{\lambda} \left[ - (M_{\lambda}^2 - N_{\lambda}^2) + \frac{1}{\rho\sqrt{A}} 2b(M_{\lambda}^2 + N_{\lambda}^2) \right. \\
\left. + \frac{1}{\rho^2 A} \left( (s^2 - b^2)(M_{\lambda}^2 - N_{\lambda}^2) + 2bs^2 \right) \right]
\end{aligned}$$

$$Y = \sum_{\lambda} \left[ s^2 + \frac{1}{\rho\sqrt{A}} 2s^2(M_{\lambda}^2 + N_{\lambda}^2) + \frac{1}{\rho^2 A} s^2 \left( -2b(M_{\lambda}^2 - N_{\lambda}^2) + s^2 - b^2 \right) \right]. \quad (\text{B.9})$$

We have checked that all these results obtained by hand correspond with the outputs of the FORM programs.

## References

- [1] P. H. Ginsparg and K. G. Wilson, Phys. Rev. **D25** (1982) 2649.
- [2] P. Hasenfratz, Nucl. Phys. **B** (Proc. Suppl.) **63** (1998) 53;  
P. Hasenfratz, V. Laliena and F. Niedermayer, Phys. Lett. **B427** (1998) 125.
- [3] H. Neuberger, Phys. Lett. **B417** (1998) 141;  
H. Neuberger, Phys. Lett. **B427** (1998) 353.
- [4] R. Narayanan and H. Neuberger, Nucl. Phys. **B443** (1995) 305;  
R. Narayanan and H. Neuberger, Phys. Lett. **B302** (1993) 62.
- [5] F. Niedermayer, Nucl. Phys. **B** (Proc. Suppl.) **73** (1999) 105.
- [6] P. Hasenfratz, Nucl. Phys. **B525** (1998) 401.
- [7] M. Lüscher, Phys. Lett. **B428** (1998) 342.
- [8] H. B. Nielsen and M. Ninomiya, Phys. Lett. **B105** (1981);  
H. B. Nielsen and M. Ninomiya, Nucl. Phys. **B185** (1981); erratum Nucl. Phys. **B195** (1982) 541.
- [9] M. Lüscher, Nucl. Phys. **B549** (1999) 295;  
M. Lüscher, Nucl. Phys. **B568** (2000) 162.
- [10] M. Lüscher, Nucl. Phys. **B** (Proc. Suppl.) **83-84** (2000) 34.
- [11] H. Neuberger, Nucl. Phys. **B** (Proc. Suppl.) **83-84** (2000) 67.
- [12] P. Hernández, K. Jansen and M. Lüscher, Nucl. Phys. **B552** (1999) 363.
- [13] H. Neuberger, Phys. Rev. **D57** (1998) 5417;  
H. Neuberger, Phys. Rev. Lett. **81** (1998) 4060;  
R. G. Edwards, U. M. Heller and R. Narayanan, Nucl. Phys. **B540** (1999) 457;  
R. G. Edwards, U. M. Heller and R. Narayanan, Phys. Rev. **D59** (1999) 094510;  
A. Bode, U. M. Heller, R. G. Edwards and R. Narayanan, “First experiences with HMC for dynamical overlap fermions”, hep-lat/9912043;  
P. Hernández, K. Jansen and L. Lellouch, “A numerical treatment of Neuberger’s lattice Dirac operator”, hep-lat/0001008;

- R. Narayanan and H. Neuberger, “An alternative to domain wall fermions”, hep-lat/0005004;  
L. Giusti, C. Hoelbling and C. Rebbi, in preparation.
- [14] Y. Kikukawa and A. Yamada, Phys. Lett. **B448** (1999) 265.
- [15] M. Ishibashi, Y. Kikukawa, T. Noguchi and A. Yamada, “One-loop analyses of lattice QCD with the overlap Dirac operator”, hep-lat/9911037.
- [16] C. Alexandrou, H. Panagopoulos and E. Vicari, Nucl. Phys. **B571** (2000) 257.
- [17] C. Alexandrou, E. Follana, H. Panagopoulos and E. Vicari, “One-loop renormalization of fermionic currents with the overlap-Dirac operator”, hep-lat/0002010, to be published in Nucl. Phys. B.
- [18] S. Capitani et al., Nucl. Phys. **B570** (2000) 393;  
S. Capitani et al., Nucl. Phys. **B** (Proc. Suppl.) **83-84** (2000) 232.
- [19] S. Capitani and G. C. Rossi, Nucl. Phys. **B433** (1995) 351.
- [20] G. Beccarini, M. Bianchi, S. Capitani and G. C. Rossi, Nucl. Phys. **B456** (1995) 271.
- [21] M. Göckeler et al., Nucl. Phys. **B472** (1996) 309;  
M. Göckeler et al., Phys. Rev. **D53** (1996) 2317.
- [22] M. Göckeler et al., Nucl. Phys. **B** (Proc. Suppl.) **53** (1997) 81;  
M. Göckeler et al., Nucl. Phys. **B** (Proc. Suppl.) **53** (1997) 896.
- [23] S. Capitani et al., “Local bilinear operators on the lattice and their perturbative renormalisation including  $O(a)$  effects”, hep-lat/9711007, in: “Deep Inelastic Scattering off Polarized Targets: Theory Meets Experiment”, Proceedings of the SPIN97 Topical Workshop, J. Blümlein, A. De Roeck, T. Gehrmann and W.-D. Nowak eds. (DESY, 1997), p. 266;  
S. Capitani et al., Nucl. Phys. **B** (Proc. Suppl.) **63** (1998) 874.
- [24] S. Capitani, M. Göckeler, R. Horsley, P. E. L. Rakow and G. Schierholz, Phys. Lett. **B468** (1999) 150;  
S. Capitani, M. Göckeler, R. Horsley, P. E. L. Rakow and G. Schierholz, Nucl. Phys. **B** (Proc. Suppl.) **83-84** (2000) 893.
- [25] S. Capitani and L. Giusti, in preparation.
- [26] S. Capitani, M. Göckeler, R. Horsley, H. Perlt, P. E. L. Rakow, A. Schiller and G. Schierholz, in preparation.
- [27] H. Kawai, R. Nakayama and K. Seo, Nucl. Phys. **B189** (1981) 40.
- [28] S. Caracciolo, P. Menotti and A. Pelissetto, Nucl. Phys. **B375** (1992) 195.
- [29] M. Lüscher and P. Weisz, Nucl. Phys. **B266** (1986) 309.